Journal of
Materials Chemistry C

Accepted Manuscript

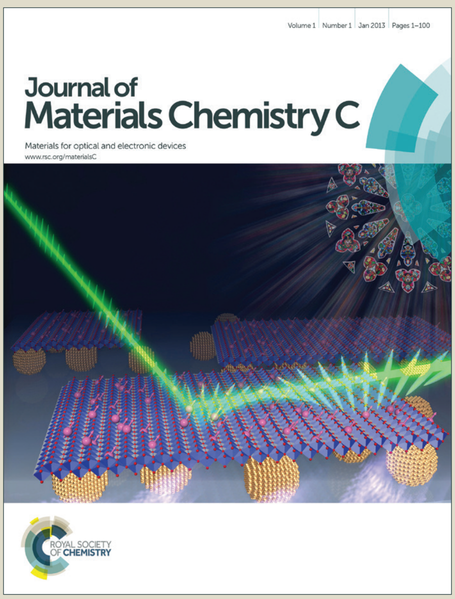

Cite this: DOI: 10.1039/c0xx00000x

www.rsc.org/xxxxxx

ARTICLE TYPE

Room temperature curable zirconium silicate dielectric ink for electronic applications

Jobin Varghese[a,b], Merja Teirikangas[a], Jarkko Puustinen[a], Heli Jantunen[a] and Mailadil Thomas Sebastian[a,b*]

Received (in XXX, XXX) Xth XXXXXXXXX 20XX, Accepted Xth XXXXXXXXX 20XX
DOI: 10.1039/b000000x

A facile formulation of room temperature curable and screen printable zirconium silicate ($ZrSiO_4$) ink has been developed. The $ZrSiO_4$ ink printed on flexible BoPET (biaxially-oriented polyethylene terephthalate) substrate showed a surface roughness of ~160 nm for a printed layer thickness of 25 µm. The screen printed $ZrSiO_4$ layer on BoPET substrate has relative permittivity of 3.01 and dielectric loss of 0.006 at 10 GHz. It showed a temperature coefficient of relative permittivity of 55 ppm/°C in the temperature range of 30-60 °C at 15 GHz. The room temperature curability, low dielectric loss, low relative permittivity, mechanical and temperature stability of microwave dielectric properties of printed $ZrSiO_4$ layer make it suitable for printed microwave applications.

Introduction

Recently, there has been an increasing demand for printing materials for the manufacture of low-cost consumer electronics. This is due to the high flexibility of the printing process providing significant advantages over conventional manufacturing processes. The printed electronic applications such as smart packages[1], flexible displays[2], distributed sensors[3,4], and antennas[5] offer the possibility of low-cost flexible devices. Different types of inks based on functional materials are required for printed electronics. This includes capacitor materials with high relative permittivity (>30), insulator layers with low relative permittivity (<5) and low melting point sealing glasses (<500 °C).[6,7] Screen printing is a simple, and low-cost manufacturing method widely used for fabrication of ceramic thick films in the range 10-100 µm.[8] The screen printing ceramic ink consists of ceramic fillers with suitable organic solvents, dispersant and binders. [9] The main challenge of the screen printing process is suitable particle dispersion to achieve uniformly thick film. Low viscosity of screen printing ink causes difficulties during printing and drying, such as dilated lines or inhomogeneous film solidity. The prevention of the so-called coffee ring effect is of high importance to achieve uniform thick film.[10] For these reason, the judicial control of the process parameters and the rheological properties of the screen printing inks are mandatory requirements.[11]

The high and low relative permittivity inks are extensively used in dynamic random access memory (DRAM) capacitors, photovoltaics and multilayer ceramic (MLC) circuits.[12-15] Recently several kinds of screen printable inks have been reported. Chang *et.al.*, have reported screen-printable P(VDF-TrFE)/PMMA/$BaTiO_3$/Silica (SII) dielectric ink for organic field-effect transistors (OFETs).[16] The epoxy/$BaTiO_3$ nano composite dielectric is reported to have capacitance of 6 nF/cm^2 with high relative permittivity of 35 at 30 kHz.[17] It has also been reported that increasing the loading level of nano powders in P(VDF-TrFE) results in relative permittivity up to 51.5.[18] Recently, Wang *et. al.* reported electrical properties of screen-printed doped ceria interlayer for IT-SOFC (Intermediate Temperature-Solid Oxide Fuel Cells) applications.[19] Despite the enormous demands, there is a great lack of published literature on the development of low permittivity and low loss screen printable inks. The above reported dielectric inks need high curing temperatures (>120 °C) and hence it limits the use of plastic substrates for printed electronic applications.

Recently Jobin *et. al.,* reported room temperature curable dielectric silica ink with low permittivity and dielectric loss.[20] The orthosilicates are predominantly covalently bonded which restricts the rattling of atoms resulting in low dielectric loss and low relative permittivity. $ZrSiO_4$ which belongs to the orthosilicate family is abundantly available in nature and is low cost. $ZrSiO_4$ is also reported as a suitable microwave substrate because of its excellent dielectric and thermal properties.[21, 22] In this paper we report the dielectric properties of room temperature curable screen printed $ZrSiO_4$ layer for high frequency applications.

Results and discussions

$ZrSiO_4$ powder analysis

Figure 1 shows the X-ray diffraction pattern and particle size analysis of processed $ZrSiO_4$ powder. The peaks of $ZrSiO_4$ can be indexed (Figure 1 (a)) based on ICDD File No: 83-1378, which indicates the absence of any secondary phases. It has a tetragonal structure and belongs to the $I4_1$/amd space group. $ZrSiO_4$ has a = 6.573 Å, c = 5.963 Å and an X-ray density of 4.7 g/cm^3. The particle size analysis was done on $ZrSiO_4$ which was preheated at 600 °C. Figure 1 (b) represents the particle size distribution of preheated $ZrSiO_4$ and the average particle size distribution is in the broad range of 500-1000 nm with an average particle size of 776 nm. The particle size and phase purity are two important parameters which control the colloidal stability of the suspension.[23, 24] The average particle size required for the screen printing application ranges 100-1000 nm depending upon the mesh size of the screen used.

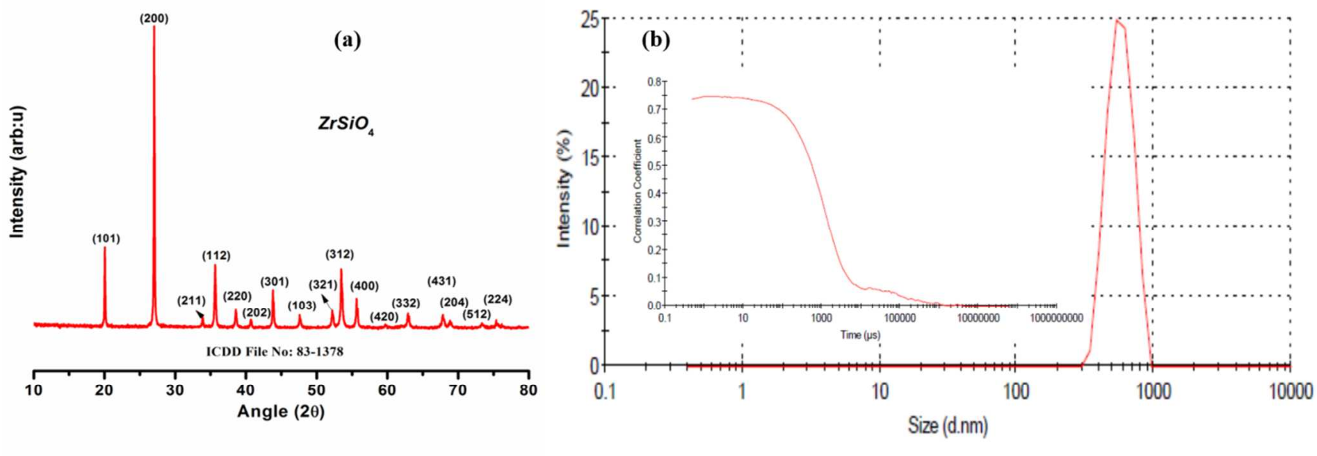

Fig. 1 (a) The X-ray diffraction pattern and (b) particle size analysis of the heat treated, ball milled and sieved $ZrSiO_4$ powder.

Formulation of screen printable $ZrSiO_4$ ceramic ink

A homogeneous and stable suspension of $ZrSiO_4$ was obtained through the use of controlled particle size, optimised composition of dispersant and binders. It was reported earlier that a suitable combination of solvent, dispersant and binder system can provide a stabilized ceramic suspension free from aggregation or phase separation.[20] The two main mechanisms for the colloid stability are steric and electrostatic stabilization. It is reported that polyvinyl butyral based ink formulation improve the printability, strength, flexibility and surface smoothness of the printed layers.[20] Long chain fatty acids present in the dispersant (fish oil) effectively dispersed the $ZrSiO_4$ ceramic particle in the organic vehicle of anhydrous xylene and ethanol mixture (1:1 ratio). The organic solvent mixture used in the present ink formulation help the room temperature curability of the ink by non-convertible coatings cure by evaporation of the solvent system without any chemical reaction.[25] The binder uniformly distribute the fillers in the polymer network.

Table 1 shows the final composition of the $ZrSiO_4$ ink. The present ink composition is based on our previous silica ink composition reported.[20] The ink consisted of 60 wt. % of $ZrSiO_4$ ceramic filler, 35 wt. % of anhydrous xylene ethanol solvent system, 1 wt. % of dispersant fish oil and 5 wt. % of polyvinyl butyral binder with respect to the filler. Generally, viscosity required for screen printing application is above 5 Pa.s at the shear rate of above 10 s^{-1} with pseudoplastic nature of suspension.[26,27] Figure 2 (a) shows the rheological characteristics of optimized $ZrSiO_4$ ceramic ink. The prepared $ZrSiO_4$ ink showed pseudoplastic nature, i.e, viscosity decreased with increasing shear rate. The formulated ink showed a viscosity of 12 Pa.s at lower shear rate of 10 s^{-1} while at a higher shear rate of 90 s^{-1} viscosity decreased down to about 3 Pa.s. The viscosity of the ink proved to be feasible for screen printing and maintained colloidal stability. In the present case $ZrSiO_4$ ceramic ink cures in less than 10 minutes depending on the atmospheric conditions.

Table 1 Composition of $ZrSiO_4$ ink

Suspension	Ink content	Ink compositions (wt. %)
Filler	$ZrSiO_4$	60
Solvents	Anhydrous xylene and ethanol (1:1)	35
Dispersant	Fish oil	1[a]
Binder	Polyvinyl butyral	5[a]

[a] With respect to filler

Inset in Figure 2 (a) shows the CSIR-emblem printed on BoPET substrate using the optimized colloidal suspension of $ZrSiO_4$. Figure 2 depicts the surface morphology of printed $ZrSiO_4$ layer on BoPET substrate at two different print strokes. Figure 2 (b) shows the single print stroke layer deposition. The mesh openings are visible in the optical image while in the double print stroke (Figure 2 (c)), the thickness of the printed $ZrSiO_4$ layer increased and hence less mesh openings were visible. Inset in Figure 2 (b, c) represents the interface of BoPET substrate and $ZrSiO_4$ layer after two print strokes. We have used a homemade screen printer with limited resolution. The resolution of the printed layer can be improved by using a standard sophisticated commercial screen printer.

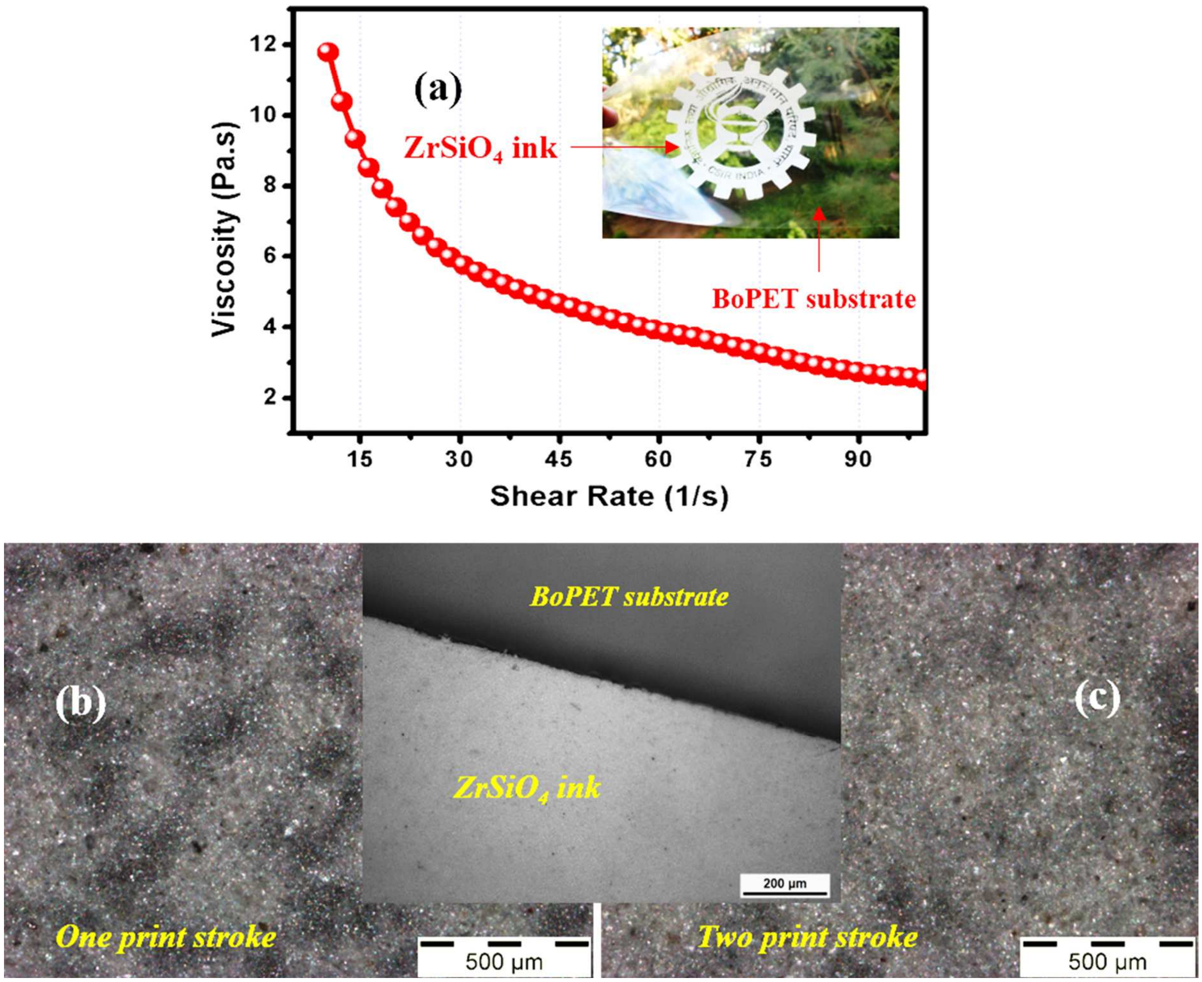

Fig.2 (a) Rheology of the final $ZrSiO_4$ ink, (b, c) Optical microscopy images of printed $ZrSiO_4$ layer.

Microstructure and surface analysis of printed layers

The adhesion test was carried out using a single printed $ZrSiO_4$ layer on BoPET film having thickness of ~12 µm. The scotch test analysis was performed on freshly printed patterns 5, 10, 15, 20, 25 and 30 minutes after printing. The scotch tape test qualitatively confirmed that the screen printed $ZrSiO_4$ layer shows good adhesion to the BoPET film even for a single print (see supporting information Figure s1). The microstructure of the screen printed $ZrSiO_4$ layer surface is shown in Figure 3 (a) which presents dense and uniform distribution of $ZrSiO_4$ particles. The microstructure is believed to originate from the low solid loading as well as the volatilization of the organic solvents. The boundary between the BoPET substrate and the $ZrSiO_4$ layer is clearly visible in the microstructure as depicted in Figure 3 (a). The $ZrSiO_4$ crystallites are distributed in the polymeric matrix as visible in Figure 3 (b). Thickness of the printed $ZrSiO_4$ layer is shown in Figure 3 (c) after double print stroke and it shows a print layer thickness of ~25 µm.

Surface roughness of the printed layers and substrates are very important in the various fabrication steps involved in the printed electronic devices.[28-30] Figure 4 (a, b) illustrates the surface roughness of the screen printed $ZrSiO_4$ layer and BoPET substrate. A more projecting and clear microstructure of the printed $ZrSiO_4$ layer surface and BoPET substrate are clear from the 3D AFM images. The average surface roughness (Ra) of screen printed $ZrSiO_4$ layer was about 160 nm and the root mean square (RMS) deviation of surface roughness (Rq) was nearly 200 nm. The Ra for BoPET substrate was of the order of 3 nm as shown in the Figure 4 (b). These parameters give the printed surface height

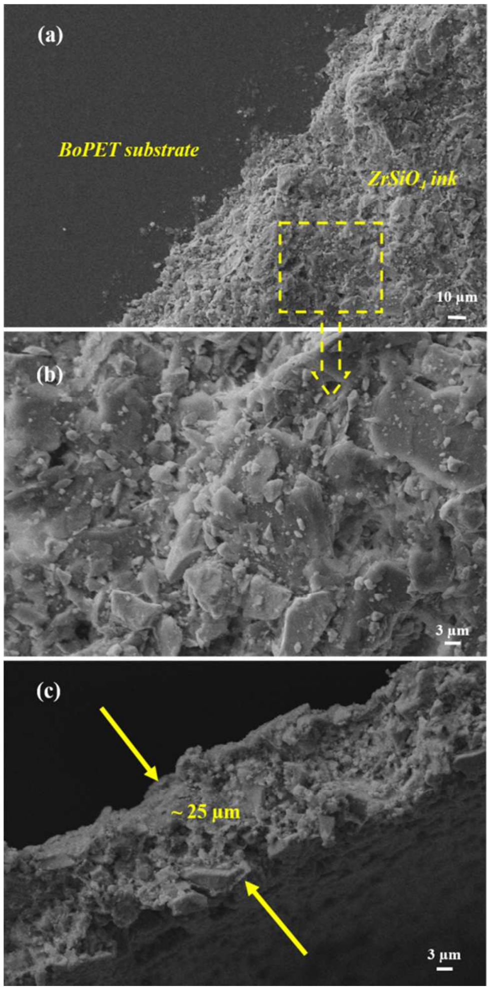

Fig.3 The SEM microstructure of the screen printed $ZrSiO_4$ layer on BoPET film (a) surface inter face (b) surface and (c) cross section of peel off $ZrSiO_4$ layer.

distribution as well as the root mean square deviation of height profile of both the surfaces. In the printed patterns, the skewness which is a measure of the variation of the surface, is -0.462. The negative value of skewness generally indicates that the surface distribution has a longer lower valley at the measurement areas in Figure 4 (a). The printed $ZrSiO_4$ layer has uneven surface distribution with considerable amount of porosity as compared to the smooth BoPET substrate. The lower positive skewness (0.249) value of BoPET substrate shows the smoothness of the substrate. The kurtosis of the topography height distribution is found to be nearly 2.97 nm which indicates the uneven surface of the printed ink. The bumpy nature with mountains and valleys on the surface of the printed $ZrSiO_4$ layer is more evident in the 3D image in Figure 4 (a). The kurtosis distribution is less than 3, the distribution curve is called platykurtoic and has relatively few high mountains and low valleys.[31] If the kurtosis distribution is greater than 3, the distribution curve is said to be leptokurtoic and has many high peaks and low valleys. The BoPET substrate has kurtosis value of 6.26 nm and it surface is leptokurtoic as shown in the Figure 4 (b) 3-D profile. The screen printed $ZrSiO_4$ layer surface is platykurtoic and is shown in the figure 4 (a) 3-D profile. The observed surface parameters are good enough for screen printing applications.

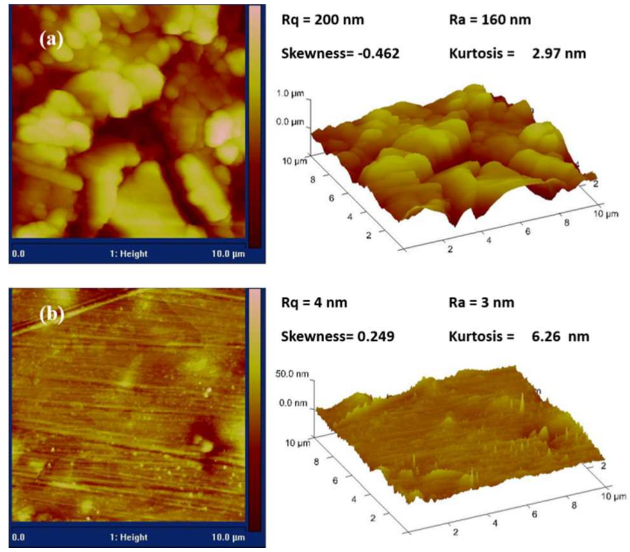

Fig.4 AFM surface roughness, 2-D and 3-D profile of the (a) screen printed $ZrSiO_4$ layer and (b) BoPET substrate.

Dielectric properties of printed patters

The $ZrSiO_4$ bulk ceramics has ε_r of 7.4 and tan δ of 0.0006 at 5 GHz.[21] The variations of relative permittivity (ε_r), dielectric loss (tan δ) and impedance (Z) of printed $ZrSiO_4$ layer on BoPET film in the radio frequency range of 600 Hz–3 MHz are shown in Figure 5. All these properties showed a decreasing trend with increasing frequency.

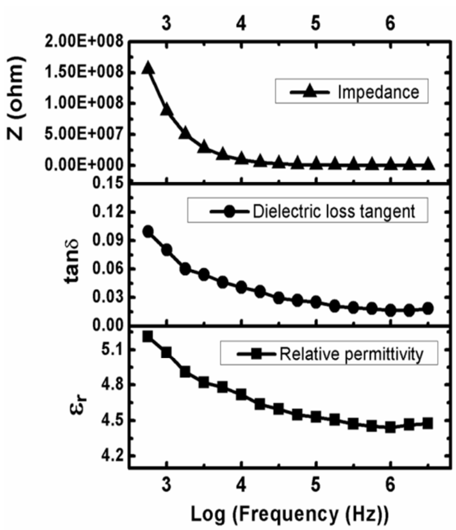

Fig.5 Dielectric properties of $ZrSiO_4$ layer on BoPET film as a function of frequency (600 Hz - 3 MHz).

Table 2 Measured dielectric properties of the BoPET film with printed $ZrSiO_4$ layer and extracted properties for the bare $ZrSiO_4$ layer at 10 GHz.

Layers	Thickness (mm)	ε_r	tanδ
BoPET Film	0.07	3.37	0.0056
Screen printed dielectric $ZrSiO_4$ layer with BoPET film	0.097	3.01	0.0058
$ZrSiO_4$ layer	0.025	2.05	0.0064

The printed $ZrSiO_4$ layer on BoPET film has ε_r of 4.5 and tan δ of 0.02 at 1 MHz. The microwave dielectric properties of screen printed $ZrSiO_4$ layer measured at 10 GHz is given in Table 2. The printed $ZrSiO_4$ layer on BoPET film shows a relative permittivity of 3.01 and dielectric loss of 0.0058 while the bare BoPET film shows relative permittivity of 3.37 and dielectric loss of 0.0056 at 10 GHz. The extracted relative permittivity and dielectric loss of printed $ZrSiO_4$ layer alone is of 2.05 and 0.0064 respectively at 10 GHz.

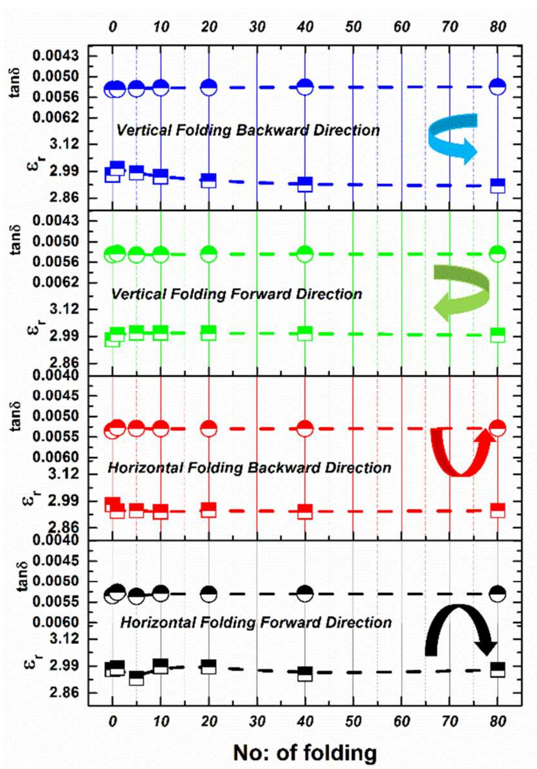

Fig.6 Effect of folding on dielectric properties of $ZrSiO_4$ layer on BoPET film at 10 GHz.

The effect of folding in horizontal, vertical and forward and backward direction on relative permittivity and dielectric loss of printed $ZrSiO_4$ layer on BoPET film at 10 GHz is shown in Figure 6. It is evident that there is not much variations in the relative permittivity and dielectric loss for various number of folding such as 0, 5, 10, 20, 40 and 80 in different directions. The small change in the relative permittivity (less than 2 %) observed after 80 folds proves its good stability versus mechanical stress. The mechanical stability (folding) of the dielectric properties are also important for the device level integration of printed electronic materials.

The values of relative permittivity and dielectric loss of printed $ZrSiO_4$ layer on BoPET film is also measured at X (8.2–12.4 GHz) and Ku band (12.4–18 GHz) frequency ranges utilizing wave guide method (Figure 7 (a)). The frequency variation of relative permittivity of printed layer is found to be nonlinear with a decreasing trend and varies from 3.40 to 3.29 in the measured frequency range of 8.2–18 GHz. The dielectric loss increases from 0.003 to 0.0057 with increase in the measured frequency range (8.2-18 GHz). However it may be noted that the relative permittivity of the printed $ZrSiO_4$ layer is lower than that of bulk $ZrSiO_4$ (7.4 at 5 GHz) [21]. This discrepancy is believed to be due to the contribution from the organics used in the formulation of colloidal $ZrSiO_4$ ink and the resultant porosity that occurred during the screen printing. The dielectric loss tangent of the printed layer increases with frequency at microwave range (8.2-18 GHz). External factors such as porosity, organics, impurities, *etc.* influence the dielectric loss behavior of the material.[32] The temperature coefficient of relative permittivity (τ_ε) is one of the critical parameters required for the stability of the signal in the printed microwave devices. The variation of relative permittivity of printed $ZrSiO_4$ layer on BoPET substrate with respect to the temperature range (25-60 ^oC) is shown in Figure 7 (b) and gives a τ_ε of 55 ppm/^oC. About 10 % variations in the relative permittivity at 10 and 15 GHz using SPDR is attributed to difference in measurement equipment and accessories used. The two different measurement methods and equipment's may attribute the 12 % variation in the relative permittivity measurement using SPDR and wave guide technique used in this study.

Methodology and characterization

Methodology

The raw material used was commercially available $ZrSiO_4$ (98 + %, 325 meshes, Sigma Aldrich, St. Louis, MO-63103 USA) powder. The $ZrSiO_4$ powder was ball milled for 24 hours followed by sieving using 25 micron mesh filter ("A-1" Sieves, Chennai, India). $ZrSiO_4$ powder was preheated at 600 ^oC for 30 minutes to remove the moisture and organic contaminants during powder processing. The solvent used for the preparation of ceramic ink was a mixture of anhydrous xylene/ethanol (Sigma Aldrich, St. Louis, MO-63103 USA). Fish oil (Arjuna Natural Extracts, Kerala, India) was used as the filler dispersant and polyvinyl butyral (Sigma Aldrich, St. Louis, MO-63103 USA) as the binder for dielectric ink preparation. The dielectric ink was prepared by ball milling of dielectric filler for 12 hours with anhydrous xylene/ethanol as the solvent and fish oil as the dispersant in an air tight Teflon bottle. This is followed by the addition of polyvinyl butyral (Butvar B – 98, molecular weight 40-70 (weight average in thousands)) binder and milled again for 12 hours. The final composition of the ceramic ink was ready for printing after the completion of the second stage of milling.

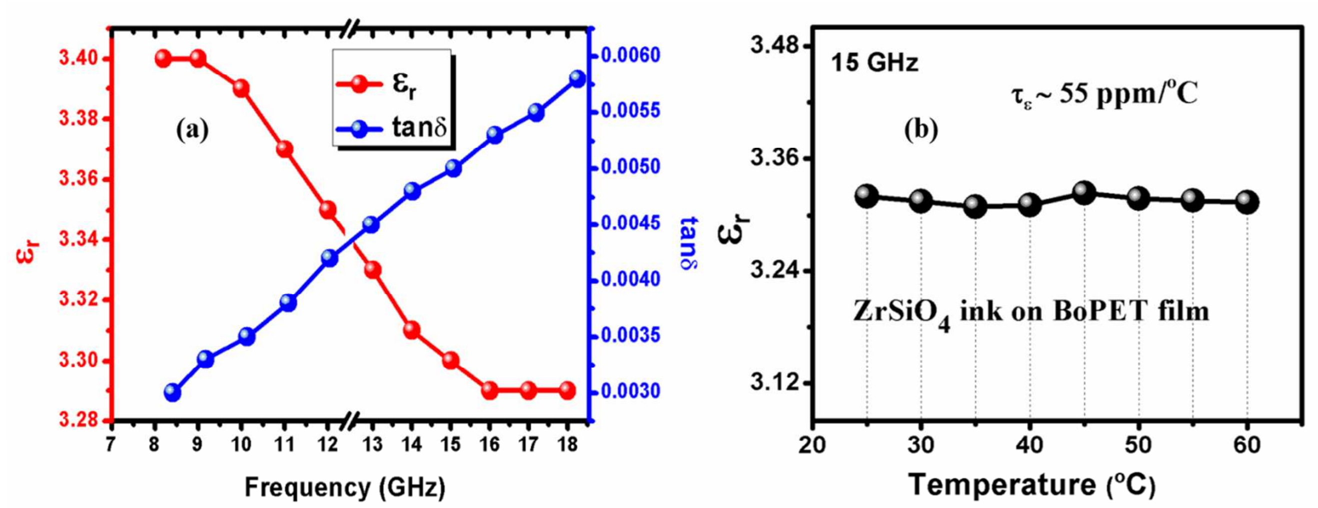

Fig. 7 (a) Dielectric properties at X and Ku band frequency range and (b) temperature variation of relative permittivity at 15 GHz of $ZrSiO_4$ layer on BoPET film.

A screen with mesh count of 325 and tightly bound to a metallic frame of dimension 220×170 mm was used as the print screen. The desired geometric pattern for printing was obtained by conventional photoresist masking technique. The flexible BoPET (biaxially-oriented polyethylene terephthalate) film was used as the printing substrate for $ZrSiO_4$ ink. Prior to printing, the screen was rinsed with the solvent mixture used in the $ZrSiO_4$ ink formulation to make the screen wet and avoid mesh blockage.

Characterization

The colloidal balance of the $ZrSiO_4$ ceramic ink was measured using rheometer (Brookfield, R/S Plus, Massachusetts, USA). The optical microscope (Leica, MRDX) was used to examine the print quality of the $ZrSiO_4$ layer. The adhesion strength of the screen printed $ZrSiO_4$ layer on BoPET substrate was measured by using scotch tape analysis recommended by ASTM Standard D3359-02 (Method B), as a standard test method for measuring adhesion. The adhesion test was carried out on freshly printed patterns after 5, 10, 15, 20, 25 and 30 minutes after printing using a Wonder 555™ self-adhesive tape followed by washing with distilled water and drying. The phase purity of the $ZrSiO_4$ ceramic fillers was studied using X-ray diffraction (XRD) (X'Pert PRO MPD X-ray diffractometer, PANalytical, Almelo, Netherlands) and the processed $ZrSiO_4$ particle size measured by Malvern particle size analyser (Zetasizer Nanoseries: ZEN 3600, Malvern Worcestershire, UK). The microstructure of printed patterns were studied using scanning electron microscopy (SEM) (JEOL JSM-5600LV, Tokyo, Japan and the surface roughness of screen printed layer over BoPET film was measured using Atomic Force Microscope (AFM) (NTEGRA, NT-MDT, Russia).

The radio frequency dielectric measurement of printed ink was measured using Hioki LCR meter (HIOKI 3532-50 LCR Hi TESTER, Japan), with sample dimension of 11 mm diameter and 1 mm thickness. The microwave dielectric properties of printed $ZrSiO_4$ layer on BoPET film and BoPET film were measured by wave guide technique for the X and Ku band frequency ranges with sample dimensions for the X band (8.2–12.4 GHz) of 22.86 ×10.8 × 0.097 mm and 15.80 × 7.90 × 0.097mm for the Ku band (12.4–18 GHz; dielectric properties were determined from the measured scattering parameters with an accuracy of 2 %) using a Vector Network Analyzer (E5071C,Agilent Technologies, Santa Clara, CA).[20, 33, 34] The microwave dielectric properties of printed $ZrSiO_4$ layer on BoPET film and BoPET film were also measured at 10 and 15 GHz using Split Post Dielectric Resonator (SPDR) (QWED, Warsaw, Poland). In this technique the total uncertainty of real permittivity does not exceed 0.5% and is possible to resolve dielectric loss tangents to approximately $5x10^{-5}$.[35] The effect of folding (bending) on microwave dielectric properties of printed $ZrSiO_4$ layer on BoPET film is also measured. The temperature variation of relative permittivity at 15 GHz was measured using the SPDR technique with sample dimension of 20 × 20 × 0.097 mm in the temperature range of 25-60 °C.

Conclusions

The present paper discusses the formulation of room temperature curable and screen printable $ZrSiO_4$ ink. The colloidal stability and room temperature curability of the ink is based on the solvent, filler, dispersant and binder compositions. The $ZrSiO_4$ ink has been screen printed on flexible substrate. The average surface roughness of the printed $ZrSiO_4$ ink is 160 nm for a printed layer thickness of ~25 µm. The screen printed $ZrSiO_4$ layer on BoPET substrate has relative permittivity of 3.01 and dielectric loss of 0.0058 at 10 GHz. The effect of folding on relative permittivity and dielectric loss shows consistent stability of the screen printed $ZrSiO_4$ layer on BoPET substrate. The relative permittivity and dielectric loss are also measured in the X and Ku band frequency ranges. The screen printed $ZrSiO_4$ layer on BoPET substrate shows a temperature coefficient of relative permittivity of 55 ppm/°C in the temperature range of 25-60 °C at

15 GHz. The room temperature curing, low dielectric loss, low relative permittivity, mechanical and temperature stability of microwave dielectric properties of printed $ZrSiO_4$ layer make it suitable for printed microwave electronic applications.

Acknowledgement

The authors are thankful CSIR, New Delhi and ERC project No:24001893 for financial support.

Notes and references

[a] *Department of Electrical Engineering, Microelectronics and Materials Physics Laboratory, University of Oulu, 90570 Finland.*
E-mail: mailadils@yahoo.com

[b] *Materials Science and Technology Division, CSIR-NIIST, Thiruvananthapuram, Kerala, India.*

1. V. Subramanian, J. M. J. Fréchet, P. C. Chang, D. C. Huang, J. B. Lee, S. E. Molesa, A. R. Murphy, D. R. Redinger, S. K. Volkman, *Proc. IEEE* **2005**, *93*, 1330.
2. A. C. Arias, S. E. Ready, R. Lujan, W. S. Wong, K. E. Paul, A. Salleo, M. L. Chabinyc, R. Apte, R. A. Street, Y. Wu, P. Liu, B. Ong, *Appl. Phys. Lett.* **2004**, *85*, 3304.
3. Y. Zhan, Y. Mei, L. Zheng, *J. Mater. Chem. C* **2014**, *2*, 1220.
4. R. Thirumalai, R. D. Mukhopadhyay, V. K. Preveen, A. Ajayagosh, *Nature Sci. Rept.* **2015**, 5, 9842.
5. I. Locher, M. Klemm, T. Kirstein, G. Tröster, *IEEE Transactions on Advanced Packaging* **2006**, *29*, 1521.
6. D. L. Hankey, A. S. Shaik, S. Vasudevan, C. S. Khadilkar, Thick film materials and process, in hybride microelectronics hand book, Editors, J. E. Sergent, C. A. Harper, McGraw-Hill, New York, **1995**.
7. R. G. Blackwell, The electronic packaging hand book, CRC and IEEE press, **2000**.
8. A. Stirini, A. Sanson, E. Mercadelli, A. Sangiorgi, L. Schiavu, *Thin Solid Films* **2013**, *545*, 537.
9. T. Siponkoski, M. Nelo, J. Perántie, J. Juuti, H. Jantunen, *Composites Part B* **2015**, *70,* 201.
10. R. D. Deegan, O. Bakajin, T. F. Dupont, G. Huber, S. R. Nagel, T. A. Witten, *Nature* **1997**, *389*, 827.
11. J. Stringer, B. Derby, *J. Eur. Ceram. Soc.* **2009**, *29*, 913.
12. J. Stringer, B. Derby, *Langmuir* **2010**, *26*, 10365.
13. S. Ducharme and A. Gruverman, Nat. Mater., 2009, 8, 9.
14. H. Kang, R. Kitsomboonloha, J. Jang, V. Subramanian, *Adv. Mater.* **2012**, *24*, 3065.
15. D. Makarov, D. Karnaushenko, O. G. Schmidt, *Chem. Phys. Chem.* **2013**, *14*, 1771.
16. X. Hou, S. C. Ng, J. Zhang, J. S. Chang, *Organic Electronics* **2015**, *17*, 247.
17. A. Rasul, J. Zhang, D. Gamota, M. Singh, C. Takoudis, *Thin Solid Films* **2010**, *518*, 7024.
18. F. A. Yildirim, C. Ucurum, R.R. Schliewe, W. Bauhofer, R.M. Meixner, H. Goebel, W. Krautschneider, *Appl. Phys. Lett.***2007**, *90*, 083501.
19. J. L. Sun, J. X. Wang, C. R. He, P. Shen, Q. Wang, H. Miao, W. G. Wang, *J. Alloy. Comp*. **2015**, *628* 450.
20. J. Varghese, K. P. Surendran, M. T. Sebastian, *RSC Adv.***2014**, *4*, 47701.
21. J. Varghese, T. Joseph, M. T. Sebastian, *Mater. Lett.* **2011**, *65*, 1092.
22. F. L. Pirkle, D. A. Podmeyer, Zircon: Origin and uses, Transactions, Society for mining, metallurgy and exploration, Inc. *292*, **1993**.
23. Y. Zeng, S. Grandner, C. L. P. Oliveira, A. F.Thunemann, O. Paris, J. S. Pedersen, S. H. L. Klapp, R-v. Klitzing, *Soft Matter*. **2011**, *7*, 10899.
24. B. J. Maranzano, N. J. Wagner, *J. Rheol.* **2001**, *45*, 1205.
25. Y. Imanaka, Multilayered low temperature co-fired ceramics (LTCC) technology, Springer, USA, 2005.
26. C. A. Harper, Handbook of thick film hybrid microelectronics, McGraw-Hill Book, Company, New York, 1974.
27. M. Lahti, S. Leppävuori, V. Lantto, *Appl. Surf. Sci.*, 1999, *142*, 367.
28. P. Oittinen, *Advances in printing Science and Technology*, Pentech, London, *15*, 344, 1980.
29. D. W. Donigian, J. N. Ishley, K. J. Wise, *TAPPI Journal*, 1997, *80*, 163.
30. R. Bollström, A. Määttänen, D. Tobjörk, P. Ihalainen, N. Kaihovirta, R. Österbacka, J. Peltonen, M. Toivakka, *Organic Electronics,* 2009, *10,* 1020.
31. E. S. Gadelmawla, M. M. Koura, T. M. A. Maksoud, I. M. Elewa, H. H. Soliman, *J. Mater. Proces. Tech.*2002, *123*, 133.
32. *M. T.* Sebastian, Dielectric materials for wireless communication. Oxford: Elsevier Science Publishers, 2008.
33. J. Varghese, M. Présumey, M. T. Sebastian, K. P. Surendran, *Mater. Chem. and Phys.* 2014, *148*, 96.
34. H. Kähäri, M. Teirikangas, J. Juuti, H. Jantunen, *J. Am. Ceram. Soc.*, 2014, *97,* 3378.
35. *J. Krupka, A. P. Gregory, O. C. Rochard, R. N. Clarke, B. Riddle, J. J. Baker,* J. Europ. Ceram. Soc.*, 2001,* 10*, 2673.*

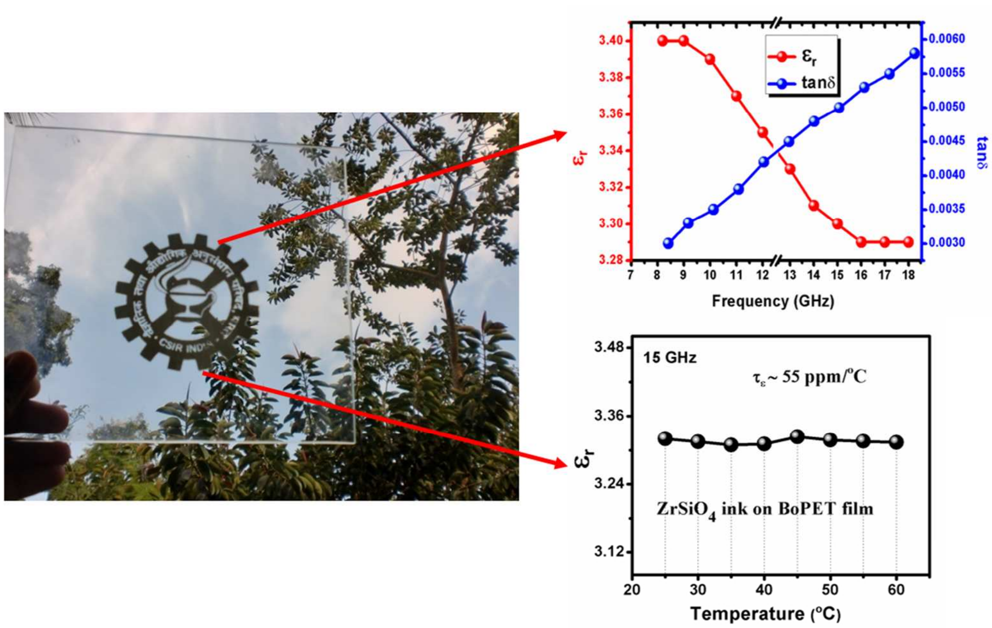

Room temperature curable ZrSiO4 ink
196x126mm (150 x 150 DPI)